ORIGINAL RESEARCH PAPER

Wet Chemical Feasible Synthesis of PPy-Nickel Oxide nanocomposites and their photocatalytic effects on Methylene Blue

*Nandini V. Iyer [1, 2], Ganesh. L. Agawane [2], Abhishek Bhapkar [1], Jayant A. Kher [2], Shekhar D. Bhame [1, *]*

[1] *Symbiosis International (Deemed University), Symbiosis Institute of Technology, Lavale, Pune-412115, India*
[2] *Department of Applied Sciences, COEP Technological University, Pune-411005, India*

ABSTRACT

In this paper, we report, the synthesis of conducting polymer nanocomposites of nickel oxide polypyrrole (NiO-PPy) doped with dodecyl benzene sulphonic acid for its application as a photocatalyst. In-situ polymerization of the pyrrole technique was employed along with oxidant ammonium persulphate and dodecyl benzene sulphonic acid as a dopant. The nanostructures were synthesized at different concentrations of NiO nanoparticles viz. 0.05 wt.%, 0.1 wt.%, 0.2 wt.% and 0.3 wt.%. The development of nanostructures was explored by Fourier Transform Infrared Spectrophotometer, Field Emission Scanning Electron Microscope, X-ray diffraction spectrometer, and electrical conductivity measurements. FTIR studies revealed a shift in the absorption band when pure PPy and NiO-PPy nanocomposites were studied, exhibiting the substantial interaction between the PPy network and the NiO. FE-SEM analysis demonstrated the consistent distribution of NiO with globular-shaped metal oxide materials in the PPy host template. The XRD studies for pure PPy revealed its amorphous nature while nanocomposites indicated the prominent NiO peaks arising from (111), (200), and (220) planes. The nanocomposites' direct electrical conductivity at room temperature was much higher than pure PPy. It was observed that the electrical conductivity for pure PPy was 0.409×10^{-5} S/cm while it substantially increased to 4.2×10^{-5} (S/cm) for 0.3% nanocomposite. The electrical studies revealed that the electrical conductivity goes on growing with increased NiO concentration and subsequently after a saturation point, more PPy encapsulates the NiO and in turn, reduces the electrical conductivity. With 0.5 g/L of 0.3% nanocomposite, the photocatalytic degradation of the Methylene-Blue dye was 84.98%.

Keywords: Conducting polymers, PPy, NiO doping, Photocatalysis, Water splitting

INTRODUCTION

Recently, material science's significant development has brought a wide variety of cutting-edge technologies to engineering. Since the last century, the materials have become multifunctional, and due to these materials needed optimization of their mechanical, chemical, physical, optical, and electrical properties. Multiple functional materials with a combination of properties are a priority [1]. Conducting polymers has received a lot of attention in the last three decades as smart materials due to their commercial significance, excellent stability in different environmental conditions, electrical conductivity, and excellent mechanical, optical, and electronic properties [2-11]. A variety of conducting polymers, including polyaniline (PANI), polyacetylene (PA), poly(p-phenylenevinylene) (PPV), polypyrrole (PPy), poly-furan (PF), poly (3,4-ethylene dioxythiophene) (PEDOT), and another polythiophene (PTh) derivative, have attracted particular attention in nanotechnology due to some of their distinct and exceptional properties. These characteristics include electrical characteristics, a conducting mechanism, a doping/undoping procedure that is reversible, tunable

chemical and electrochemical characteristics, and ease of processability [3-11]. Among the several available polymers, Polypyrrole (PPy) has been the subject of many studies due to its unique properties such as versatility of synthesis, relatively high electrical conductivity, and outstanding mechanical strength [12]. Due to potential uses as well as scientific issues, inorganic nanocrystalline materials have received a lot of attention. These materials' nanoscale dimensions provide them with a variety of physical and chemical characteristics [3]. The growing interest in nanocomposites made of PPy (an organic material) and NiO (an inorganic nanomaterial) stems from the fact that these materials' characteristics differ significantly from that of PPy and the equivalent NiO nanocomposites due to their interfacial interactions. Sonavane et al. prepared PPy–NiO composites by using a chemical bath deposition technique and PPy's electrochemical properties were improved. [13] It has been shown that NiO nanocomposite with PPy-Au coating has improved electrocatalytic capabilities. [14] Jia et al. employed a de-deposition technique for polypyrrole (PPy) and Au on NiO nanobeads host matrix and prepared nanocomposites for electroanalyses uses [15]. To examine thermal stability, Roy et al. created a PAni/NiO nanocomposite using different surfactants [16]. Nalage et al. synthesized nickel oxide and added polypyrrole matrix nanoparticles using a solid-state reaction process [17]. Though there are several reports on the synthesis of nanocomposites in various ways, numerous amounts of researchers have prepared at relatively higher concentrations of NiO nanoparticles [18-20]. Reports have shown that the electrical conductivity and stability diminish if a substantially higher amount of NiO is doped in the electrode materials [18-21]. Therefore, to the authors' knowledge, for the first time in this study, we have prepared nanocomposites at very low concentrations of NiO like 0.05% to 0.3%. This indicates the possibility of preparing to conduct polymers for photocatalytic applications at a very low cost, with a simple and benign technique.

Due to the increased usage of dyes, pollution from dye wastewater has recently become a serious environmental issue [22]. When these substances are dumped into bodies of water without being treated, the ecology may suffer and an ecological imbalance may result. These dyes are carcinogenic and mutagenic, which enter the food cycle and cause harm to animals and human beings [23]. Methylene Blue (3,7-bis (dimethylamine)-phenothiazine-5-methylthionionium chloride) is a thiazine dye. It has many applications as a dye and medicine [24].

Semiconductor oxides like TiO_2, ZnO, SnO_2, and NiO have drawn researchers' attention to the degradation of organic compounds due to their superior photocatalytic efficacy. when doped in the polypyrrole host matrix, excellent biocompatibility, competitive prices, greater chemical, and physical properties, and a strong ability to decompose organic pollutants into harmless species such as CO_2, H_2O, etc. Furthermore, optimum electron transfer in the visible spectrum adequately occurs between the valance band and conduction band in the presence of polypyrrole as a host matrix [24-25]. It is well known that semiconductor oxide deteriorates by photocatalytic means when exposed to UV and visible light. This enables holes to form in the conduction band, producing an $(e-)$-hole $(h+)$ pair, when excited electrons located in the valence band move into the latter. Hydroxyl radicals $(\bullet OH)$ are generated when the potential of the hole (h^+) reacts with the adsorbed hydroxide ions or water molecules on the oxide surface. Superoxide ion $(\bullet O_2^-)$ is created when the molecular oxygen is reduced by the potential of the electron (e^-). The toxic compounds are degraded into safe products by the hydroxyl radical and superoxide ions. Later, the photocatalytic activity is reduced because the holes (h^+) and electrons (e^-) swiftly recombine with one another. [25]

In this research, to the best of the authors' knowledge, very low-concentration nickel oxide nanoparticles were added to the polypyrrole matrix to create polypyrrole hybrid nanocomposites. This was accomplished by employing an in-situ chemical polymerization approach using the dopant 4-Dodecyl benzene sulfonic acid to incorporate a low concentration of nickel oxide nanoparticles into the polypyrrole matrix. The use of the NiO-PPy hybrid nanostructured materials was explored as a photocatalyst in the

24

J. Water Environ. Nanotechnol., 8(1): 23-33 Winter 2023

photocatalytic decomposition of Methylene Blue dye under Ultraviolet irradiation in the laboratory.

EXPERIMENTAL DETAILS
Chemicals used

Pyrrole was purchased from Kemphasol, World of Chemicals, India. Nickel (II) Oxide nanoparticles of the size of <50nm were purchased from Aldrich Chemistry, India.4-Dodecyl benzene sulfonic acid was purchased from Aldrich Chemistry, India, and Ammonium persulfate was purchased from Fischer Scientific, India.

Synthesis of Polypyrrole-NiO Hybrid Nanocomposites

Nickel oxide polypyrrole (NiO-PPy) hybrid nanostructured materials were prepared by the technique of in-situ synthetic crosslinking using pyrrole and ammonium persulphate (APS) in the molar ratio of 1:1.5M and 0.05 M 4-Dodecyl benzene sulphonic acid (DBSA). NiO nanoparticles of the size < 50nm with varying concentrations of 0.05,0.1,0.2 and 0.3wt.%were used. The NiO nanoparticles were added to 0.05M 4-dodecyl benzene sulphonic and stirred for 15 minutes using a magnetic stirrer for uniform mixing.1M pyrrole prepared in ethanol was added dropwise to the homogeneous mixture of NiO nanoparticles and DBSA at 0°C with constant stirring and the addition was completed in 15 minutes.1.5 M aqueous solution of APS was added with constant stirring and the addition was completed in 30 minutes. The process was carried out at 0 °C and the reaction time varied was 4hrs.,8 hrs.,12 hrs., and 16 hrs. After obtaining a black precipitate, it was cleaned and filtered multiple times with ethanol and deionized water to remove any oligomers and potential contaminants, and it was then allowed to air dry for 24 hours at room temperature. To create fine PPy powder, the resultant black powder was further ground in an agate pestle and mortar. The PPy powder was further characterized.

Photocatalytic degradation Studies

In a photochemical reactor, Methylene Blue dye (MB) was photo-catalytically degraded utilizing PPy-NiO nanocomposite. By dispersing 25 mg and 50 mg of the PPy, PPy-NiO nanocomposites in 100 ml of 10 mg/l of MB pigment solution, the equilibrium between the adsorption and desorption for the catalyst and the dye was attained. In complete darkness, this mixture was

stirred for 10 minutes. When the photocatalyst and dye solution was homogeneous, the solution was constantly stirred under a UV light source (254 nm). Until 120 minutes had passed, 10 mL of the dye mixture was removed at 20-minute intervals and centrifuged. With the aid of a UV-Vis absorption spectrophotometer, the absorbance was measured.

Characterization

PPy, NiO, PPy-DBSA, and NiO-PPy-DBSA hybrid composites were examined using Fourier transform infrared spectroscopy (FT-IR) (Model: Shimadzu-IR affinity 1S). X-ray diffraction (XRD) experiments were carried out utilizing (Model: Rigaku Miniplex 600). The patterns were captured using Cu K radiation (k=1.5406) in the 2-theta range of 10-80°. The XRD spectra were assessed by correlating the observed peaks with the reference pattern provided by the JCPDS file. Using a field emission scanning electron microscope (FE-SEM), the surface morphology of PPy, NiO, PPy-DBSA, and NiO-PPy-DBSA hybrid nanostructures was investigated (Model: Carl Zeiss India Ltd., Sigma IV). The FE-SEM images were used to calculate the grain size. Using two probes, the conductivity measurements were performed (Keithley 2000).

RESULTS AND DISCUSSION
Structural studies

Fig. 1 depicts the XRD spectra of PPy and NiO-PPy hybrid nanocomposites (0.05, 0.1, 0.2, and 0.3 wt.%). The XRD spectrum of PPy reveals a broad hump at 22°. The nickel oxide X-ray diffraction results match the Joint Committee on Powder X-ray diffraction Standards (JCPDS) file No. 73-1519 exactly., which portrays a cubic phase of NiO [17].

The XRD spectra of the NiO-PPy nanostructures (0.05, 0.1, 0.2, and 0.3 wt.%) (Fig. 1) exhibit all the essential NiO diffraction peaks as well as the broad PPy peak at 22°, which is the unique peak of PPy. The hump of PPy weakens as the amount of NiO nanoparticles increases. All the NiO-PPy XRD spectra show prominent peaks arising from the planes (111), (200), (220), and (311) which are the signature peaks of NiO crystal lattices aligned in PPy polymer chains [JCPDS No. 73-1519][17]. Furthermore, as the reaction duration lengthens, the conspicuous

J. Water Environ. Nanotechnol., 8(1): 23-33 Winter 2023

25

Table 1. Crystallite size was calculated by using Scherrer's equation.

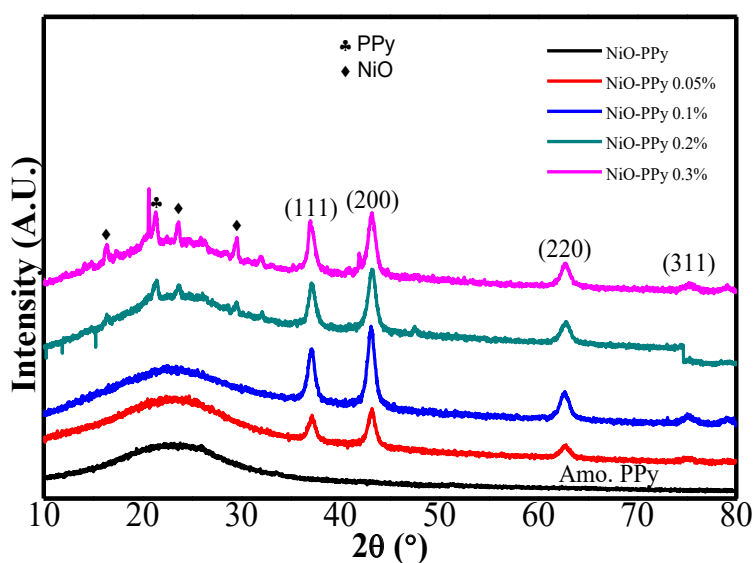| Sample No.	The average crystallite size (nm)	Error (±)
Pure PPy	Amorphous, No peak	0
0.05	11.67	0.2
0.1	8.34	0.3
0.2	6.48	0.2
0.3	8.35	0.4

Fig. 1. XRD spectra of pure PPy and NiO-PPy nanocomposites

NiO peaks are decreased, showing successful NiO incorporation in the polypyrrole matrix due to the lower concentration of NiO utilized in the research.

For the crystallite size calculations, the Scherrer equation was used on the XRD spectra. The crystallite size was calculated as given below and shown in Table No. 1.

$$D = K \lambda /(\beta \cos\theta) \tag{1}$$

Where D is the average size of crystallites (nm), K is the crystallite form factor (a fair approximation is 0.9), λ is the X-ray wavelength of Cu Kα source 0.15418 nm, β is the X-ray diffraction peak's full width at half maximum (FWHM) in radians, and θ is the Braggs' angle in degrees. Table 1 shows the computed average crystallite size values.

Surface Morphological investigations

Fig. 2 depicts the FE-SEM micrographs of PPy, NiO nanostructures, and Polypyrrole-NiO (0.05, 0.1, 0.2, and 0.3 wt.%) studied nanocomposites. The surface morphology of the NiO-PPy (0.05,0.1,0.2 and 0.3 wt.%) hybrid nanocomposite powder show mostly uniform circular, square, few rosettes and occasionally nanospheres crystals of PPy with increasing concentrations of NiO. The surface morphology shows overgrown clusters Fig.2. With the increase in the reaction time the crystals are smaller, and an amorphous and flaky matrix is observed.

Grain Size

The grain size was calculated from the FE-SEM images Fig. 3. The grain size first increases from 102 nm to 230 nm with an increase in NiO concentration from 0% to 0.05%. It then decreases to 73.59 nm and further increases to 104.4 nm with increased NiO Concentration. Overall, the grain size decreases at 0.3% NiO concentration which is beneficial for the high surface-to-volume ratio of NiO/PPy conducting polymers for photocatalytic applications.
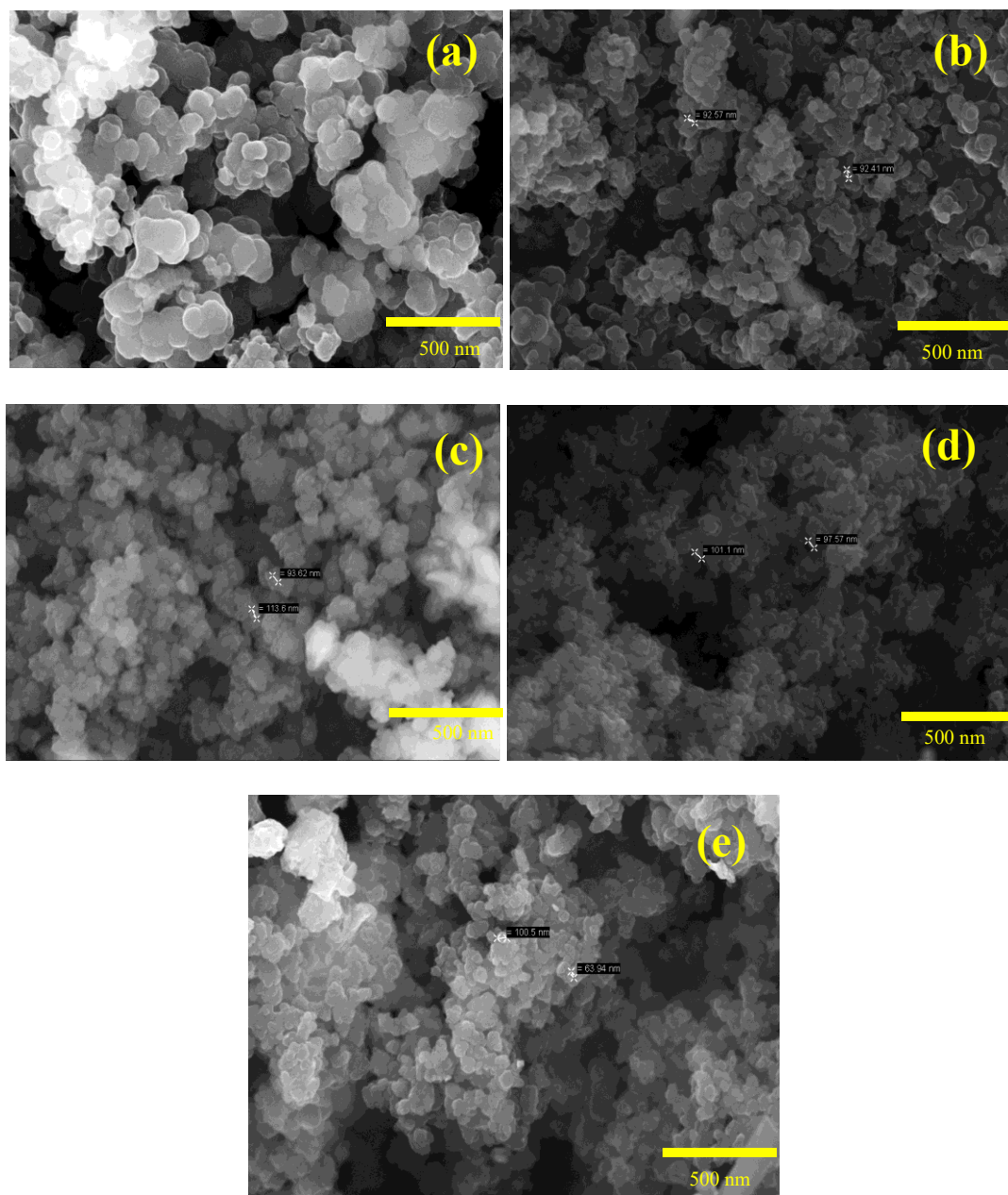
Fig. 2. FE-SEM images of pure PPy (a) and NiO-PPy (b-e) nanocomposites

Fourier Transform Infrared Spectroscopy Analysis

The FTIR spectra of the PPy and NiO-PPy at 0.05, 0.1, 0.2, and 0.3 wt.% are shown in Fig. 4 (a,b). The FTIR spectrum of PPy shows characteristic peaks at 1557.5 cm^{-1} which arises from pyrrole ring C=C deformation vibration, N–C stretching band observed at 1200.4 cm^{-1}, stretching vibration for C–C bond was observed at 1367.5 cm^{-1}. All these peaks slightly shifted to a higher wavenumber for the NiO-PPy nanocomposite samples which proved that a systematic alignment of NiO crystals in PPy chains occurred. These FTIR results are consistent with the structural and morphological studies.

Electrical Conductivity Studies

The electrical conductivity is shown in Table 2. The electrical conductivity of NiO-PPy enhances with an enhancement of the concentration of the NiO nanostructures

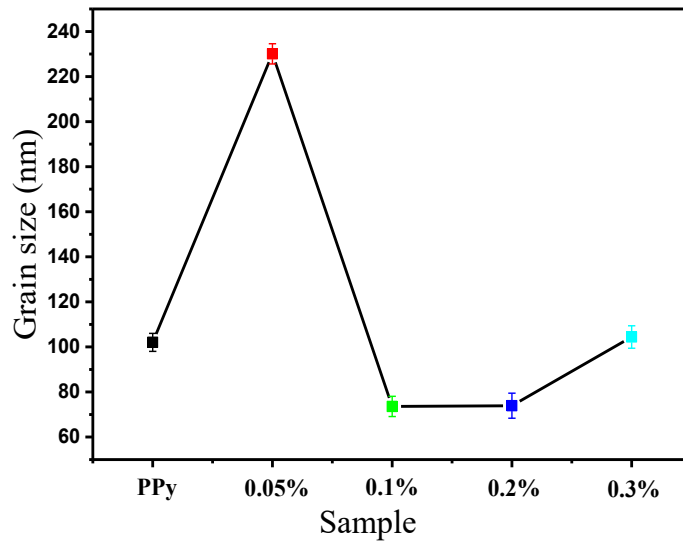*J. Water Environ. Nanotechnol., 8(1): 23-33 Winter 2023*

27

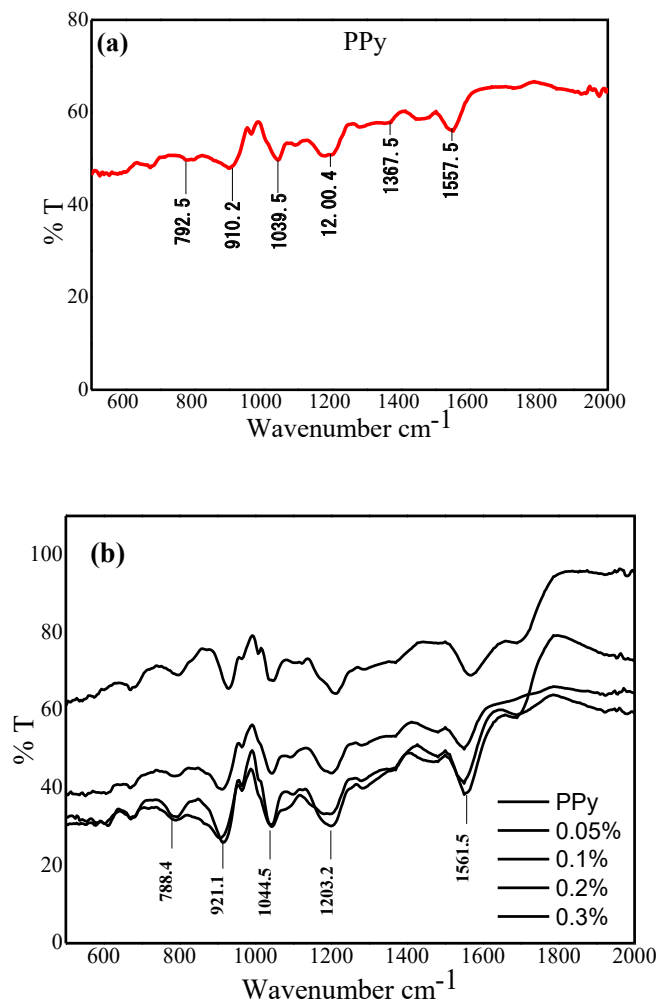Fig. 3. Grain size graph of pure PPy and NiO-PPy nanocomposites

Fig. 4. FT-IR spectra of pure PPy (a) and NiO-PPy nanocomposites (b)

Table 2. Various properties of NiO-PPy hybrid nanocomposites for reaction time 4 hrs.

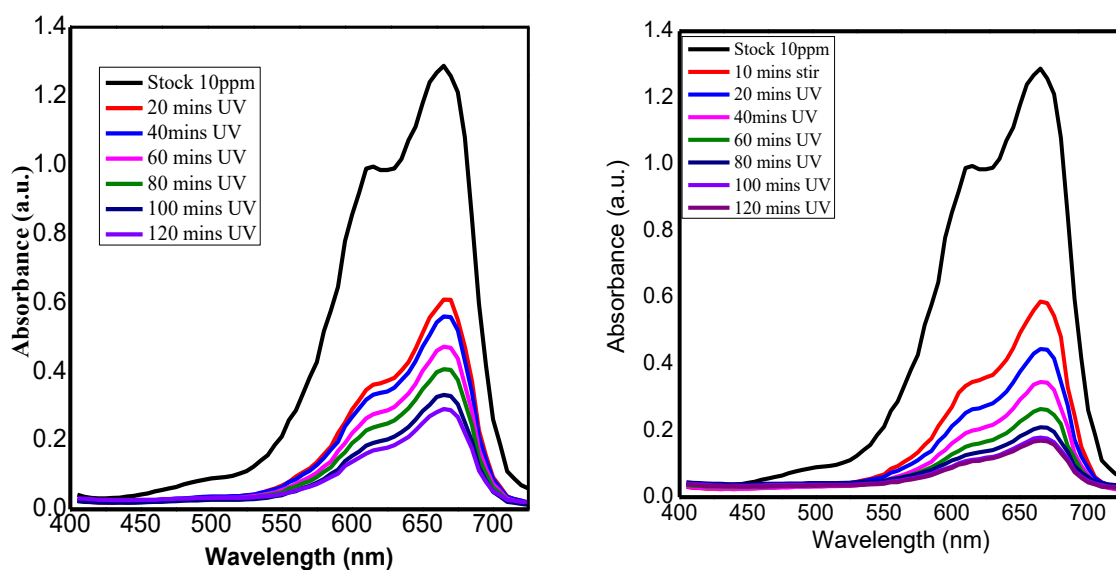| Sr. No.	Composition	Grain Size (nm)	Conductivity σ ×10⁻⁵ (S/cm)
1	PPy	102.04	0.409
2	NiO-PPy (0.05%)	230.08	1.21
3	NiO-PPy (0.1%)	73.59	0.049
4	NiO-PPy (0.2%)	73.92	1.99
5	NiO-PPy (0.3%)	104.41	4.20

Fig. 5. The absorption spectra of the Methylene blue solution in presence of NiO-PPy catalyst under solar light irradiation.

from 0.05% to 0.3% at the reaction time of 4hrs. and is high as compared to the particle loading of 10-50% used by other researchers [18]. There is no trend observed in the electrical conductivity with the increase in the reaction time and this is due to the lower concentration of NiO nanoparticle loading and the coating and shielding of PPy.

The NiO and NiO-PPy studied nanostructured compounds are P-type semiconductors with a substantial quantity of free-charge carriers responsible for conduction. The intensity of free-charge carriers rises in tandem with the NiO concentration. The conductivity of the PPy–NiO hybrid nanostructures enhanced due to e⁻ from the polar O_2^- terminated NiO nanostructures and the Polypyrrole chains.

Photocatalytic Studies

Fig. 5 (a, b) shows the photocatalytic activities of NiO nanoparticles obtained via Methylene blue degradation under UV irradiation. Briefly, 100 ml of 10 mg/l Methylene Blue dye solution was thoroughly combined with 25 mg and 50 mg NiO catalyst. The suspension was kept in the dark to minimize the effect of adsorption. The suspension is then kept under irradiation with stirring. The degraded dye was collected during the irradiation at regular intervals of 20 minutes and further centrifuged. The photocatalytic breakdown of Methylene blue was studied by recording the absorbance using a UV-Vis spectrophotometer. Fig. 5 (a) shows that when 25 mg PPy-NiO nanoparticles are exposed to light, degradation of Methylene blue in the aqueous medium increases as the reaction time increases, and 76.65% degradation took place. The degradation of Methylene blue significantly increased at 50 mg PPy-NiO to 84.98% (Fig. 5 (b)). These results undoubtedly reveal that an increased concentration of NiO nanoparticles plays a key role as a photocatalyst in the degradation of Methylene blue from the aqueous medium. These findings also indicate that PPy has helped NiO in establishing

J. Water Environ. Nanotechnol., 8(1): 23-33 Winter 2023

29

Table 3. Rate constant calculations for 25 mg and 50 mg NiO-PPy hybrid composites.

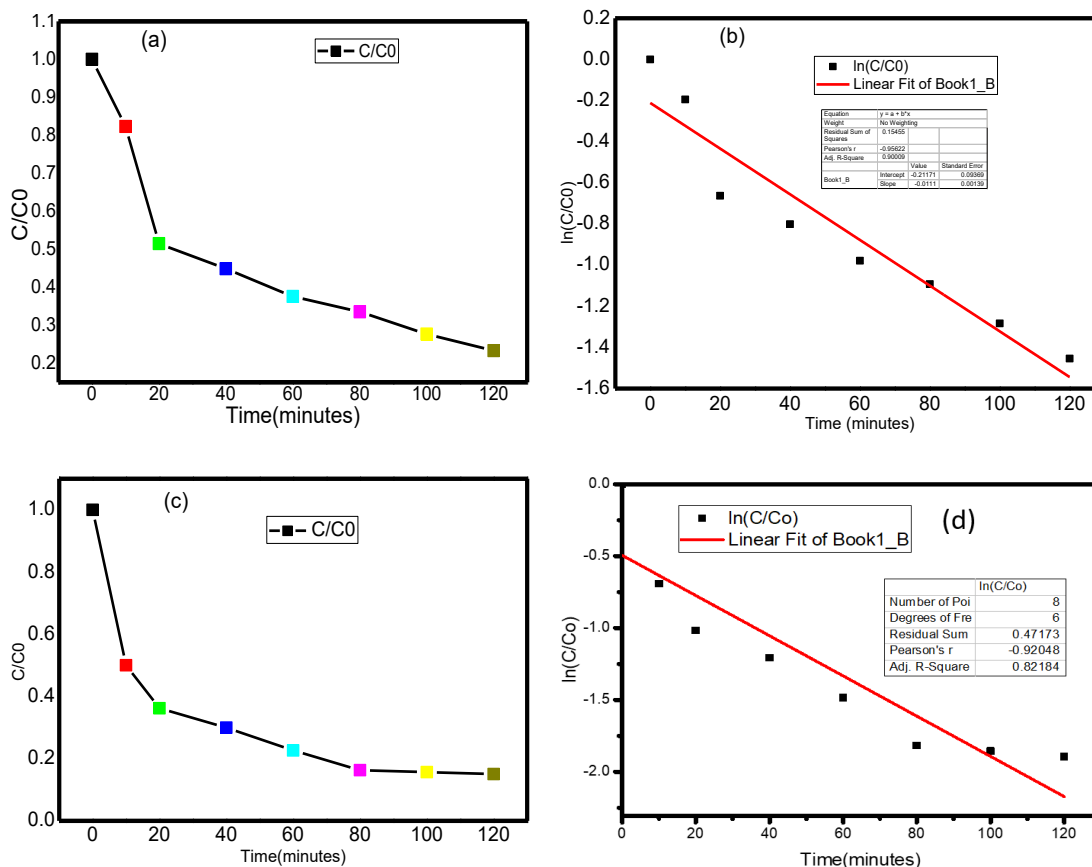| Sample	Pearson's r Value	Adj R Square Value	K (Rate constant)
PPy-NiO-25mg+10ppm MB	-0.956	0.9	0.010886
PPy-NiO-50mg+10ppm MB	-0.92	0.821	0.020122

Fig. 6. Graphs for r and R square factor for 25 mg (a,b) and 50 mg PPy- NiO (c,d)

good contact between the photogenerated holes and OH⁻ or H_2O thus facilitating the formation of hydroxyl radicals.

Further, we calculated the order of reaction by using kinetic studies. The calculations for rate constant are shown in Fig. 6 (a,b,c,d) and summarized in Table. 3 for 10 ppm dye concentration with 0.25 and 0.5 g/L catalyst. These two sets of experiments show that when NiO-doped PPy composite material is used it shows a perfect first-order reaction as only one variant is done over here. For the rest of the two materials, it does not show a perfect rate constant value. These findings reveal that the composite material of NiO-doped PPy is better than other samples and possesses enhanced stability.

Reaction mechanism

Fig. 7 depicts a realistic mechanism for dye degradation with a PPy-NiO catalyst. 84.98% of the Methylene Blue dye molecules in the aqueous solution are disintegrated by the PPy-NiO nanocomposite. Following are some possible explanations for how NiO nanoparticles affect PPy photocatalytic activity: Under UV photons, the d-orbital of NiO in the conducting band interfaces chemically with the lowest unoccupied molecular orbital of polypyrrole inside the PPy-NiO nanocomposite. The conduction band of NiO approaches the lowest unoccupied molecular orbital of PPy as just a response to these electronic interactions, and electrons are pumped into the
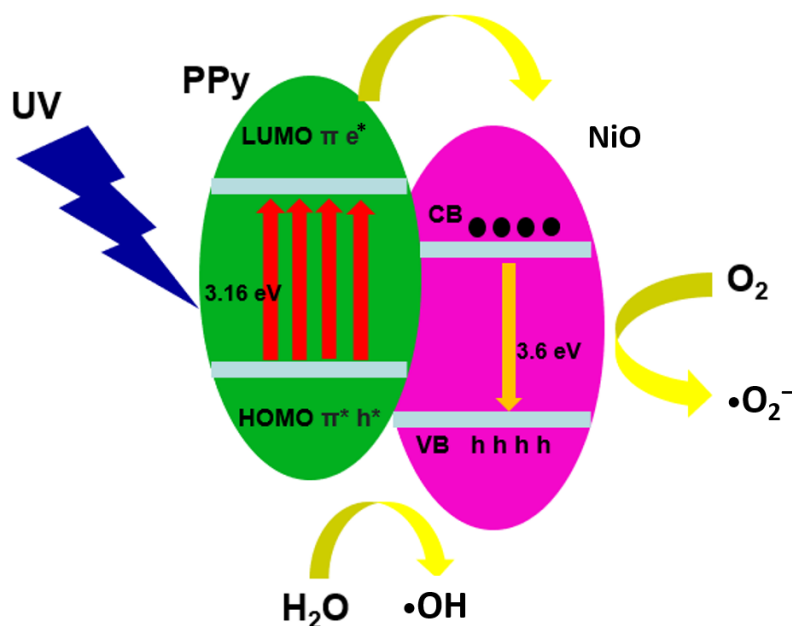
Fig. 7. Mechanism of photodegradation for PPy-NiO catalyst under UV light.

conduction band of NiO from the least unoccupied molecular orbital of PPy. The divided electrons and holes in PPy's lowest vacant molecular orbital and highest occupied molecular orbital may interact with the pollutant's oxygen (O_2) and water molecule to create superoxide radicals ($\bullet O^{2-}$) and hydroxyl radicals ($\bullet OH$), respectively. Reactive oxygen and hydroxide radicals are potent reducing and oxidizing agents that have the potential to dissolve MB's complex chemical linkages. However, NiO nanoparticles augment PPy's surface area, which may maximize the likelihood that the catalyst and light will interact, speeding up the oxidation process [26]. Additionally, NiO can act as an electron transport layer, making the passage of a photoinduced electron from PPy to NiO easier, allowing NiO to prevent PPy electron-hole pairs from recombining and thereby increasing its photocatalytic efficiency [27-30].

CONCLUSIONS

In summary, an in-situ, simple approach was employed for the preparation of NiO-PPy nanocomposite materials for photocatalytic application. We observed a change in the lattice constants of NiO when it is encapsulated in the PPy host matrix which was evidenced by a shift of 2 values towards the higher side. Surface morphology investigations demonstrated homogenous dispersion of NiO in PPy host polymer chains.

FTIR analysis revealed a shift of PPy bands towards a higher wavenumber after doping NiO nanoparticles. The electrical conductivity studies revealed higher conductivity values due to the electron hopping conduction mechanism. It is concluded that at extremely low NiO doping concentrations, the electrical conductivity values for the prepared NiO-PPy nanocomposites when compared with the literature are significantly higher. The NiO-PPy nanocomposite degrades 84.98% of Methylene Blue dye molecules when exposed to UV irradiation and a perfect first-order reaction was observed. These findings show that the synthesized nanocomposite can be used as a competent photocatalyst for the elimination of MB dye. Interestingly, this synthetic approach may be used to create NiO-doped PPy conducting polymers, confirming the ecologically friendly route.

J. Water Environ. Nanotechnol., 8(1): 23-33 Winter 2023

31

CONFLICT OF INTEREST

The authors declare no conflict of interest.

RESEARCH DATA POLICY AND DATA AVAILABILITY STATEMENTS

Scholars who choose to employ the information described in the publication for non-commercial objectives while maintaining participants' privacy will have free access to the resources listed in the publication as well as any requisite original data.

AUTHOR CONTRIBUTION

"All authors contributed to the study conception and design. Material preparation, data collection, and analysis were performed by Nandini V. Iyer, Ganesh L. Agawane, Abhishek Bhapkar, Jayant Kher, and Shekhar Bhame. The first draft of the manuscript was written by Nandini V. Iyer and all authors commented on previous versions of the manuscript. All authors read and approved the final manuscript."

CONFLICT OF INTEREST

The authors declare no conflict of interest.

REFERENCES

[1] Shukla, Uddeshya and Garg, Kamal. Journey of smart material from composite to shape memory alloy (SMA), characterization and their applications-A review. Smart Materials in Medicine, 4 (2023), 227-242. https://doi.org/10.1016/j.smaim.2022.10.002

[2] Abu-Sari, Suleiman M., Patah, Muhamad Fazly Abdul, Ang, Bee Chin, and Daud, Wan Mohd Ashri Wan. A review of polymerization fundamentals, modification method, and challenges of using PPy-based photocatalyst on perspective application. Journal of Environmental Chemical Engineering, 10 (2022), 108725. https://doi.org/10.1016/j.jece.2022.108725

[3] Shanmugam, Mariyappan, Augustin, Ashil, Mohan, Sathya et al. Conducting polymeric nanocomposites: A review in solar fuel applications. Fuel, 325 (2022), 124899. https://doi.org/10.1016/j.fuel.2022.124899

[4] Samtham, Manopriya, Singh, Diwakar, Hareesh, K., and Devan, Rupesh S. Perspectives of conducting polymer nanostructures for high-performance electrochemical capacitors. Journal of Energy Storage, 51 (2022), 104418. https://doi.org/10.1016/j.est.2022.104418

[5] Bahuleyan, B. K., Ramesan, M. T., Mavinkere Rangappa, Sanjay, Parameswaranpillai, Jyotishkumar, Yashas Gowda, T. G., Siengchin, Suchart, and Seydibeyoglu, M. Ozgur. 15 - Conducting polymers and their composites with different nanoparticles. In Nanoparticle-Based Polymer Composites. Woodhead Publishing, 2022.

[6] Song, Zhen, Ma, Yihui, Morrin, Aoife, Ding, Caifeng, and Luo, Xiliang. Preparation and electrochemical sensing application of porous conducting polymers. TrAC Trends in Analytical Chemistry, 135 (2021), 116155.

https://doi.org/10.1016/j.trac.2020.116155

[7] Chen, Xiao, Liu, Peipei, Liu, Congcong et al. Microstructure control for high-capacitance polyaniline. Electrochimica Acta, 391 (2021), 138977. https://doi.org/10.1016/j.electacta.2021.138977

[8] Stejskal, J. Sapurina, I. Trchova. M, Polyaniline nanostructures and the role of aniline oligomers in their formation, Prog. Polym. Sci. 35 (2010),1420-1481. https://doi.org/10.1016/j.progpolymsci.2010.07.006

[9] Picciani, Paulo H. S., Shimizu, Flavio Makoto, Olimpio, Quelle G., Michel, Ricardo C., and Narayan, Roger. Sensing Materials: Organic Polymers. In Encyclopedia of Sensors and Biosensors (First Edition). Elsevier, Oxford, 2023. https://doi.org/10.1016/B978-0-12-822548-6.00038-8

[10] Heydari Gharahcheshmeh, M. and Gleason, K. K. Texture and nanostructural engineering of conjugated conducting and semiconducting polymers. Materials Today Advances, 8 (2020), 100086. https://doi.org/10.1016/j.mtadv.2020.100086

[11] Phan, Samantha and Luscombe, Christine K. Recent Advances in the Green, Sustainable Synthesis of Semiconducting Polymers. Trends in Chemistry, 1 (2019), 670-681. https://doi.org/10.1016/j.trechm.2019.08.002

[12] Mohanapriya, M. K., Deshmukh, Kalim, Ahamed, M. Basheer, Chidambaram, K., and Khadheer Pasha, S. K. Influence of Cerium Oxide (CeO2) Nanoparticles on the Structural, Morphological, Mechanical and Dielectric Properties of PVA/PPy Blend Nanocomposites. Materials Today: Proceedings, 3 (2016), 1864-1873. https://doi.org/10.1016/j.matpr.2016.04.086

[13] Chavan, Utkarsh D., Prajith, P., and Kandasubramanian, Balasubramanian. Polypyrrole based cathode material for battery application. Chemical Engineering Journal Advances, 12 (2022), 100416. https://doi.org/10.1016/j.ceja.2022.100416

[14] Inamdar, Hajeebaba K., Ambika Prasad, M. V. N., and Sasikal, M. Synthesis and characterization of polypyrrole/ NiO doped Nanocomposites (NCs) for Dielectric studies. Materials Today: Proceedings, 5 (2018), 22652-22656. https://doi.org/10.1016/j.matpr.2018.06.640

[15] D. Jia, Q. Ren, L. Sheng, F. Li, G. Xie, Y. Miao, Preparation and characterization of multifunctional polypyrrole-Au coated NiO nanocomposites and study of their electrocatalysis toward several important biothiols, Sens. Actuators B 160 (1) (2011) 168. https://doi.org/10.1016/j.snb.2011.07.028

[16] Saha Roy, Hemshankar, Mominul Islam, Md., Yousuf A. Mollah, M., and Abu Bin Hasan Susan, Md. Polyaniline-NiO Nanocomposites as Dielectric Materials. Materials Today: Proceedings, 5 (2018), 15267-15276. https://doi.org/10.1016/j.matpr.2018.05.005

[17] S.R. Nalage, S.T. Navale, V.B. Patil, Polypyrrole-NiO hybrid nanocomposite: Structural, morphological, optical, and electrical transport studies, Measurement 46 (2013), 3268-3275. https://doi.org/10.1016/j.measurement.2013.06.049

[18] H. K. Inamdar, B.C. Sridhar, M. Sasikal, M.V.N. Ambika Prasad, Structural and Optical properties of Polypyrrole/NiO Doped Nanocomposites, Journal of Nanoscience and Technology 4 (2018) 400-401. https://doi.org/10.30799/jnst.113.18040305 https://doi.org/10.30799/jnst.112.18040308

[19] H. Vijeth, S.P. Ashokkumar, L. Yesappa, M. Vandana, H.

Devendrappa, Hybrid Core-Shell nanostructure made of Chitosan incorporated Polypyrrole Nanotubes decorated with NiO for All-Solid-State Symmetric Supercapacitor Application, Electrochimica Acta 354 (2020) 136651. https://doi.org/10.1016/j.electacta.2020.136651

[20] Zhang, Lin, Wang, Xingchao, Huang, Yudai et al. Rational design of bamboo mat-like 3D Ni foam@ NiO@PPy nanoarray electrode for binder-free, high-loading and high-areal capacity lithium storage. Journal of Alloys and Compounds, 874 (2021), 159957. https://doi.org/10.1016/j.jallcom.2021.159957

[21] Sarah Umeera Muhamad, Nurul Hayati Idris, Hanis Mohd Yusoff, M.F. Md Din, S.R. Majid, In-situ encapsulation of nickel nanoparticles in polypyrrole nanofibers with enhanced performance for supercapacitor, Electrochimia Acta 249 (2017) 9-15. https://doi.org/10.1016/j.electacta.2017.07.174

[22] Ancy, K., Bindhu, M. R., Bai, Jeslin Sunitha, Gatasheh, Mansour K., Hatamleh, Ashraf Atef, and Ilavenil, S. Photocatalytic degradation of organic synthetic dyes and textile dyeing waste water by Al and F co-doped TiO2 nanoparticles. Environmental Research, 206 (2022), 112492. https://doi.org/10.1016/j.envres.2021.112492

[23] Katwal, Rishu, Kothari, Richa, Pathania, Deepak, Singh, Lakhveer, and Mahapatra, Durga Madhab. Chapter 10 - An overview on degradation kinetics of organic dyes by photocatalysis using nanostructured electrocatalyst. In Delivering Low-Carbon Biofuels with Bioproduct Recovery. Elsevier, 2021. https://doi.org/10.1016/B978-0-12-821841-9.00005-0

[24] Oladoye, Peter Olusakin, Ajiboye, Timothy Oladiran, Omotola, Elizabeth Oyinkansola, and Oyewola, Olusola Joel. Methylene blue dye: Toxicity and potential elimination technology from wastewater. Results in Engineering, 16 (2022), 100678. https://doi.org/10.1016/j.rineng.2022.100678

[25] Alagarasi, A., Rajalakshmi, P. U., Shanthi, K., and Selvam, P. Solar-light driven photocatalytic activity of mesoporous nanocrystalline TiO2, SnO2, and TiO2-SnO2 composites. Materials Today Sustainability, 5 (2019), 100016. https://doi.org/10.1016/j.mtsust.2019.100016

[26] Moharana, Aiswarya, Kumar, Anupam, Thakur, Ankush et al. Chapter 6 - Role of nanostructured metal oxides in photocatalysis: An overview. In Nanostructured Photocatalysts. Elsevier, 2021. https://doi.org/10.1016/B978-0-12-823007-7.00010-9

[27] J. Hu, J. Ma, L. Wang, H. Huang, Synthesis, and photocatalytic properties of LaMnO3-graphene nanocomposites. J. Alloy. Compd. 583 (2014), 539-545. https://doi.org/10.1016/j.jallcom.2013.09.030

[28] T.W. Kim and S.J. Park, Preparation of flower-like TiO2 sphere/reduced graphene oxide composites for photocatalytic degradation of organic pollutants. J. Solid State Chem. 239 (2016), 91-98. https://doi.org/10.1016/j.jssc.2016.04.010

[29] Xu et al. One-pot¬ hydrothermal synthesis of SrTiO3-reduced graphene oxide composites with enhanced photocatalytic activity for hydrogen production. J. Mol. Catal. A: Chem. 423 (2016), 70-76. https://doi.org/10.1016/j.molcata.2016.05.025

[30] J. Hu and H. Huang, Preparation of LaMnO3/ graphene thin films and their photocatalytic activity. J. Rare Earth. 32 (2014) 1126-1134. https://doi.org/10.1016/S1002-0721(14)60193-9

J. Water Environ. Nanotechnol., 8(1): 23-33 Winter 2023

33